Scaling up of Growth, Fabrication, and Device Transfer Process for GaN-based LEDs on H-BN Templates to 6-inch Sapphire Substrates

Phuong Vuong, Tarik Moudakir, Rajat Gujrati, Ashutosh Srivastava, Vishnu Ottapilakkal, Simon Gautier, Paul L Voss, Suresh Sundaram, Jean-Paul Salvestrini, Abdallah Ougazzaden

Scaling up of Growth, Fabrication, and Device Transfer Process for GaN-based LEDs on h-BN Templates to 6-inch Sapphire Substrates

Phuong Vuong, Tarik Moudakir, Rajat Gujrati, Ashutosh Srivastava, Vishnu Ottapilakkal, Simon Gautier, Paul L. Voss, Suresh Sundaram, Jean Paul Salvestrini & Abdallah Ougazzaden[*]

P. Vuong, R. Gujrati, A. Srivastava, V. Ottapilakkal, P. L. Voss, S. Sundaram, J. P. Salvestrini, A. Ougazzaden
CNRS, Georgia Tech – CNRS IRL 2958, 2 rue Marconi, 57070 Metz, France.
P. Vuong, S. Sundaram, J.P. Salvestrini
Georgia Tech Europe, 2 rue Marconi, 57070 Metz, France.
T. Moudakir, S. Gautier
Institut Lafayette, 2 rue Marconi, 57070 Metz, France.
R. Gujrati
Georgia Institute of Technology, Woodruff School of Mechanical Engineering, Atlanta, GA 30332-0250, USA.
A. Srivastava, P.L. Voss, S. Sundaram, J.P. Salvestrini, A. Ougazzaden
Georgia Institute of Technology, School of Electrical and Computer Engineering, Atlanta, GA 30332-0250, USA.
E-mail: abdallah.ougazzaden@georgiatech-metz.fr

Abstract

We demonstrate the growth of hexagonal boron nitride (h-BN) and van der Waals (vdW) epitaxy of blue multi-quantum well (MQW) GaN-based LED heterostructures on 6-inch sapphire substrates using metal-organic chemical vapour deposition (MOCVD). We discuss challenges associated with the growth of large surface h-BN and the subsequent vdW epitaxy of GaN-based LED heterostructures. To overcome these challenges, we controlled the spatial uniformity of the growth temperature, optimized the slope of temperature variations during the growth and cooling process, and managed the surface temperature during switching of gas flows. With these adaptations, high quality GaN-based LED heterostructures were grown on h-BN without any spontaneous delamination. The GaN-based LED devices were then fabricated on a 6-inch sapphire wafer, which were lifted off as a membrane and transferred to a flexible copper support. These GaN-based LED devices emitted bright blue illumination with an electroluminescence peak at 437 nm. This scaling up of growth, lift-off, and transfer can lead to the commercialization of GaN-

based LEDs on h-BN template on 6-inch sapphire substrates, with a process compatible with current modern equipment for the fabrication of LEDs and electronic devices.

1. Introduction

vdW epitaxy of three-dimensional (3D) materials on two-dimensional (2D) layers (vdW 3D/2D) has progressed rapidly over the last decade, attracting tremendous attention, especially for III-Nitrides, where new pathways have been opened for optoelectronic/electronic nitride devices and their applications [1–5]. The vdW 3D/2D approach offers unique advantages compared to conventional 3D/3D epitaxy. The weak vdW interactions between the III-Nitrides heterostructures and 2D layered materials enable different buffer and device designs because it allows the strain due to large lattice and thermal mismatches to relax elastically without the generation of additional dislocations and defects [6,7]. In addition, with simple sticky holders such as tapes, polydimethylsiloxane (PDMS), or metal, the III-Nitride heterostructures can be mechanically detached over a large surface area from its substrate and transferred as membranes to arbitrary carriers [8,9].

Hexagonal boron nitride (h-BN) can become the 2D material of choice for III-Nitride heterostructures [10]. It exhibits a good stability at high temperature, an excellent compatibility with III-Nitride growth conditions and growth systems (MOCVD, MBE, CVD), and can be grown on various types of substrates [11,12]. Since the pioneering demonstration of LEDs on h-BN by Kobayashi's group [8], significant advances have been made, particularly for the fabrication of different optoelectronic devices and their transfer to diverse foreign substrates. Special efforts have been made for vdW growth on large surfaces, which is necessary for the commercialization of this technology [13–17]. Our group has successfully demonstrated vdW application on 2-inch and 4-inch sapphire substrates [18–20].

One important challenge for h-BN based vdW growth on large surface areas is the spontaneous delamination that occurs during growth, cooling, or device fabrication. The weak vdW bonding force that exists between the substrate and h-BN layers cannot handle the stress generated by the differences in thermal expansion between them. An additional challenge encountered when scaling up the growth to 6-inch substrates is wafer bow, which becomes an

awkward problem during epitaxial growth of 6-inch substrates. At this size, curvature of the substrate at high temperatures creates a non-uniform interspace between the substrate and the susceptor, which causes surface temperature deviations across the wafer leading to poor film quality and device performance. It also leads to significant indium (In) content variation in the InGaN/GaN MQWs resulting in strong variations in emission wavelength. We found that vdW growth scaling to 6-inch wafers is more complicated than for 2-inch or 4-inch wafers and it requires careful attention to growth conditions. To the best of our knowledge, no results for h-BN growth and subsequent vdW epitaxy have been reported on full 6-inch or larger wafers.

In this study, we report the growth of a 6-inch GaN-based LED heterostructures on 2D h-BN templates using MOCVD. We first study the growth and characterizations of 20 nm thick h-BN on 6-inch sapphire substrates. Then, vdW epitaxy of GaN-based LED epilayers was carred out on 3 nm thick h-BN on full 6-inch sapphire substrates, resulting in the emission of photoluminescence at an average wavelength of 427 nm with a standard deviation across the wafer less than 2%. We then fabricated GaN-based LED devices on a full wafer and report current-voltage (I-V) characterization and electroluminescence (EL). Additionally, we demonstrated the lift-off of these LEDs and their transfer to a flexible copper carrier. These promising results show that h-BN assisted vdW epitaxy can be successfully scaled up to 6-inch sapphire substrates, with the possibility of re-using substrates as we have demonstrated with 2-inch wafers [21].

2. Results and Discussions

2.1. Growth of 2D h-BN on 6-inch sapphire substrate

As a key stao of vdW 3D/2D, we first investigated the growth of 20 nm h-BN layers on 6-inch sapphire substrates to gain a deeper understanding of the quality of our h-BN materials. 20 nm thickness was chosen because it provides sufficient thickness for further structural and morphological characterizations. The visual appearance of a 20 nm thick h-BN grown on 6-inch sapphire substrate is shown in Fig.1a. The wafer is transparent, homogeneous, and exhibits no signature of delamination. The crystal structure of 20 nm thick h-BN was characterized using HR-XRD 2θ-ω scans, as displayed in Fig. 1b, showing the presence of clear symmetric diffraction

peaks at 25.6° which correspond to the (002) crystal planes. The lattice constant c of the h-BN film was calculated to be 0.692 nm, which is in agreement with reported value for 20 nm thick h-BN grown on 2-inch sapphire substrates [22]. To verify the uniformity of the h-BN film, SEM was performed at five equally spaced spots along the radial line from the centre of the wafer to its outer edge. The wrinkled morphology, as shown in Fig. 1c, is observed at all these five spots, and corresponds to the standard morphology of 20 nm thick h-BN grown on 2-inch sapphire substrate. As previously reported [17,23], the formation of wrinkles in h-BN on sapphire is attributed to the difference in thermal expansion coefficients (TECs) between the two materials. The presence of the wrinkles serves as an indicator of 2D layered BN.

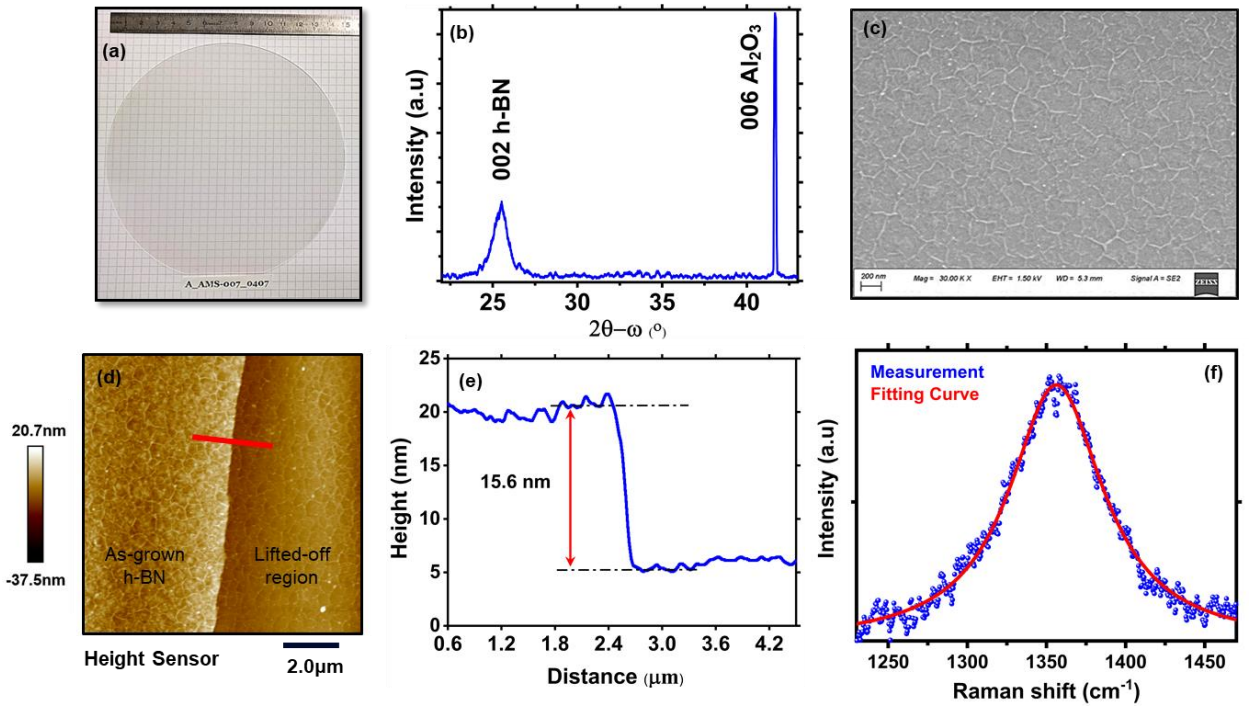

Figure 1: (a) Picture of as grown 20 nm h-BN on 6-inch sapphire substrate, (b) HR-XRD 2θ-ω scan of as grown 20 nm h-BN on 6-inch sapphire substrate, (c) SEM image of as grown 20 nm h-BN on 6-inch sapphire substrate, (d,e) AFM image and the profile measurement along the red line in the picture (d), and (f) Raman spectrum of h-BN on the lifted-off region shown in Fig.1d.

We also checked the suitability of h-BN film as a release layer for GaN-based LED heterostructures by testing a simple mechanical lift-off method using scotch tape. The AFM image, shown in Fig. 1d, demonstrate that the h-BN layer can be easily detached from its substrate over a large surface area as observed via AFM image of the sample after lift-off process. A measurement of the step between the lifted-off region and as grown surface revealed a difference of 15.6 ± 1 nm

(Fig. 1e). We estimate that a residual h-BN layer of approximately 5 nm thickness remains on the sapphire substrate, as evident from the less pronounced wrinkles of the lifted-off portion in the Fig. 1d, indicating that the lift-off occurs between h-BN layers, which are held together only by the weak vdW force. This confirms growth of continuous layered h-BN on 6-inch sapphire substrate, and hence should be possible to separate the full 6-inch GaN-based LED heterostructures fabricated on h-BN, which will be presented in the subsequent section. In addition, the Raman spectrum of the remaining 5 nm h-BN layer obtained from the lift-off region exhibited a peak at about 1360 cm^{-1} (Fig. 1f), which is attributed to the E_{2g} vibrational mode involving the out-of-plane motion of nitrogen atoms relative to the boron atoms. The full width at half maximum (FWHM) of the peak is measured at 72 cm^{-1}. In case of 20 nm thick h-BN (as presented in Supplementary Material), the peak position increases to 1375 cm^{-1} and the FWHM slightly increases to 76 cm^{-1}. These variations in peak position and FWHM are directly correlated with the thickness of the h-BN layer, which differs between the lifted-off and non-lifted-off regions.

2.2. Growth of GaN-based LED heterostructures on 2D h-BN/6-inch sapphire substrate

Prior to growing the full 6-inch GaN-based LED heterostructures, we performed a growth of n-GaN layer on 3 nm h-BN using a n-AlGaN interfacial buffer layer to mitigate the wetting issues associated with n-GaN growth on h-BN [24]. The HR-XRD ω-2θ scan conducted on the n-GaN/n-AlGaN grown on h-BN layers (Fig. 2c, blue spectrum) showed two distinct diffraction peaks at 17.28° and 17.42°, which correspond to the (002) reflections of the wurtzite GaN and the buffer layer wurtzite AlGaN, respectively. Additional details regarding this template can be found in the supplementary materials. Following this buffer layer, the GaN-based LED heterostructures, consisting of the MQWs and p-GaN layer, were grown on the n-GaN/n-AlGaN/h-BN template.

As mentioned earlier, delamination during the epitaxial growth or cooling process is a major challenge in the vdW growth of GaN-based LED heterostructures on h-BN on large surface area. One of the reasons is the rapid temperature variation during heating and/or cooling, which can increase mechanical stresses within the wafer due to the wafer thermal inertia and phase shift which generate a thermal gradient across the entire 6-inch wafer [25]. Good crystalline quality h-BN needs to be grown at high temperature (1280°C in our case), n-GaN around 1100°C and InGaN around 700°C, so for 6-inch wafers the effect of temperature changes between h-BN growth and

subsequent layer growth are more pronounced. Another reason is the switch of carrier gases, between hydrogen (H_2) with high thermal conductivity (482 mW/mK at 700°C [26]) and nitrogen (N_2) with low thermal conductivity (64 mW/mK at 700°C [27]), used for the growth of different layers of GaN-based LED heterostructures on h-BN, which causes a sudden change of surface temperature of the wafer and hence a thermal shock. As an example of these effects, Fig 2a shows abrupt delamination of the entire 6-inch GaN-based LED heterostructures grown on h-BN. The inset of Fig. 2a shows the transformation of the delaminated LED heterostructures to the multiple scroll forms.

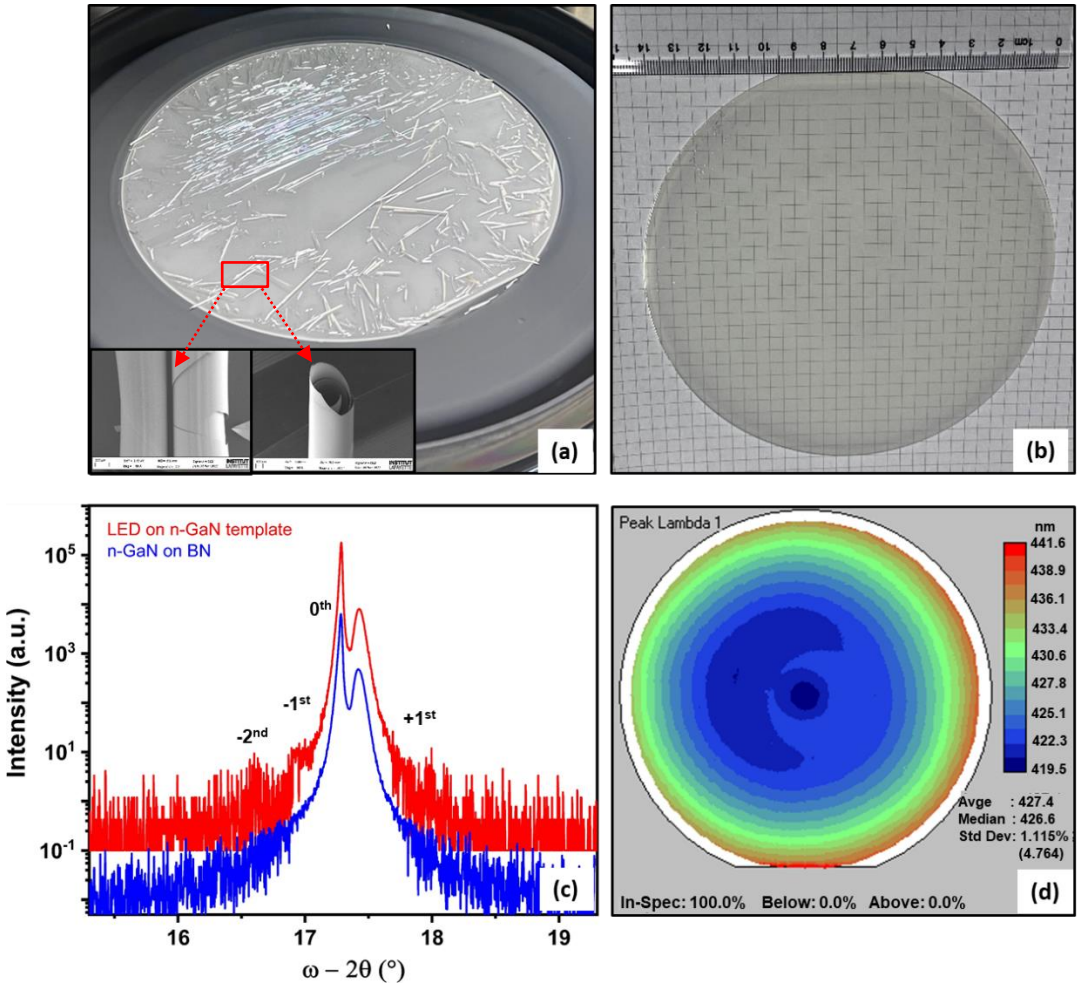

Figure 2: (a) Image of the abrupt delamination of the GaN-based LED heterostructures grown on h-BN/6-inch sapphire substrate. Inset in (a): SEM zoom of LED heterostructure/h-BN scrolls, (b) Image of delamination-free LED heterostructures growth on h-BN/6-inch sapphire substrate, (c) HR-XRD ω-2θ scan and (d) PL Map of LED heterostructures grown on n-GaN/n-AlGaN/h-BN on 6-inch sapphire substrate.

To overcome these issues, we carefully controlled the spatial uniformity of the temperature during growth by optimizing the 3 zone heaters of our growth chamber, decreased the slope of temperature changes between h-BN, n-GaN, and InGaN growth temperatures by diminishing the ramping rate of 20°C per minute steadily, and managed the surface temperature during gas flow switching between H_2 and N_2 by gradually injecting a mixture of H_2/N_2 gases before switching to 100% N_2 or H_2. The gas flow switching process was completed in approximately 300 seconds, allowing for a smooth transition between the two gas phases. The temperature control was based on real-time of in situ reflectance, curvature measurements and temperature profile over full 6-inch wafer, which were obtained from Aixtron's ARGUS monitor and LayTec's EpiCurve-TT in-situ monitor. As a result, we were able to achieve uniform, delamination-free GaN-based LED heterostructures growth on h-BN, as shown in Fig. 2b. From the curvature measurements during our GaN-based LED growth, there is almost a linear relation between temperature and stress as the curvature is proportional to the average stress. The crystalline quality of the GaN-based LED heterostructures and the correlation between the In composition and strain distribution in InGaN/GaN MQWs were evaluated using HR-XRD measurements. Intense diffraction peaks were observed from the n-GaN and n-AlGaN epilayers, as well as the first and second order of the InGaN/GaN MQWs, in the (002) HR-XRD ω-2θ scan for the GaN-based LED heterostructures, as seen in Fig. 2c (red spectrum). The In composition and the thickness of the InGaN MQWs were found to be 12% and 2.5 nm, respectively, as determined from the fitted peaks. Photoluminescence (PL) mapping across the entire 6-inch wafer was performed as shown in Fig. 2d. The PL map demonstrates a uniform emission wavelength of 427 nm with standard deviation less than 2% and an average FWHM of approximately 40 nm. It is worth mentioning that a blue light emission was observed, before fabrication process, from the wafer using two probes and by injecting a weak current.

Accurate information on wafer bow is critical for successful device fabrication processes. For this reason, a 3D profilometer was used to measure the 3D profile map of the wafers over an area of 74 mm * 100 mm prior to device fabrication. The results, presented in Fig. 3, indicate that the depth between the bottom-most and top-most points was measured to be 32 µm, 46 µm, and 37 µm for plain sapphire substrate, GaN-based LED heterostructures on sapphire, and GaN-based LED heterostructures on h-BN/sapphire, respectively. Two noteworthy points arise from our study. Firstly, the growth of GaN-based LED heterostructures on h-BN/sapphire results in a

reduced bow when compared to GaN-based LED heterostructures on sapphire. Secondly, we observed an interesting phenomenon where the 3D profile map of the GaN-based LED heterostructures grown on h-BN/sapphire displayed a warped topology that deviated from the shape of the planar sapphire substrate, unlike the 3D map of the GaN-based LED heterostructures grown on sapphire, which conformed to the substrate shape. This observation represents a novel finding, and it suggests that the growth of GaN-based LED heterostructures on h-BN/sapphire is not governed by the sapphire substrate curvature. We postulate that the bowing effect of 6-inch (and beyond) of the GaN-based LED heterostructures could be improved by adjusting the uniformity of the temperature during growth. Our study indicates that the use of a thin h-BN buffer layer on large surfaces (6-inch and above) can effectively minimize the stress and bow of the GaN-based devices grown on various substrate types, thus significantly improving their performance.

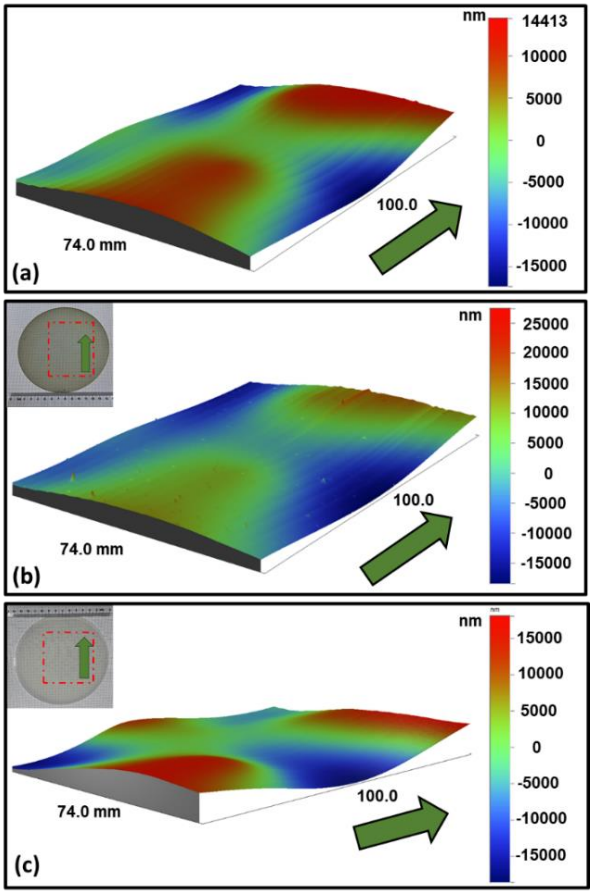

Figure 3: 3D profile map of (a) 6-inch sapphire substrate, (b) GaN-based LED heterostructure grown on 6-inch sapphire substrate, and (c) GaN-based LED heterostructure grown on h-BN/6-inch sapphire substrate.

2.3. Optical and electrical characterizations of LED devices on h-BN/6-inch sapphire substrate

The grown GaN-based LED heterostructures on h-BN/6-inch sapphire template was processed to fabricate devices. Fig. 4a shows full wafer image at an intermediate process step while Fig. 4b shows binocular image of the final processed device. Fig. 4c and 4d show the far field and near field images, respectively of the processed LED devices of square shape upon current injection. Fig. 4e shows the I-V characteristics of one of the fabricated LEDs which indicates rectifying characteristics, with a threshold voltage of around 3.0 V. The forward voltage is high and likely due to high series resistance. This high series resistance is due to the crystalline quality of both p-GaN and n-GaN layers. The low growth temperature of the p-GaN layer and the growth of the n-GaN layer on top of a low crystalline quality AlGaN buffer layer led indeed to poorly conductive layers and partially Schottky contacts. The peak emission wavelength of the LED, from the electroluminescence spectrum (EL), was measured to be 437 nm, as shown in Fig. 4f, which is consistent with the previous PL measurements. The EL intensity was found to increase with increasing current injection, as expected for a well-functioning LED device. External quantum efficiency of the LEDs was not measured because the contact design of our fabricated device is not suitable for this measurement. Indeed, most of the device area is covered by contact pads, and thus only a small part of the emitted light can be collected leading to very poor EQE value which is not representative.

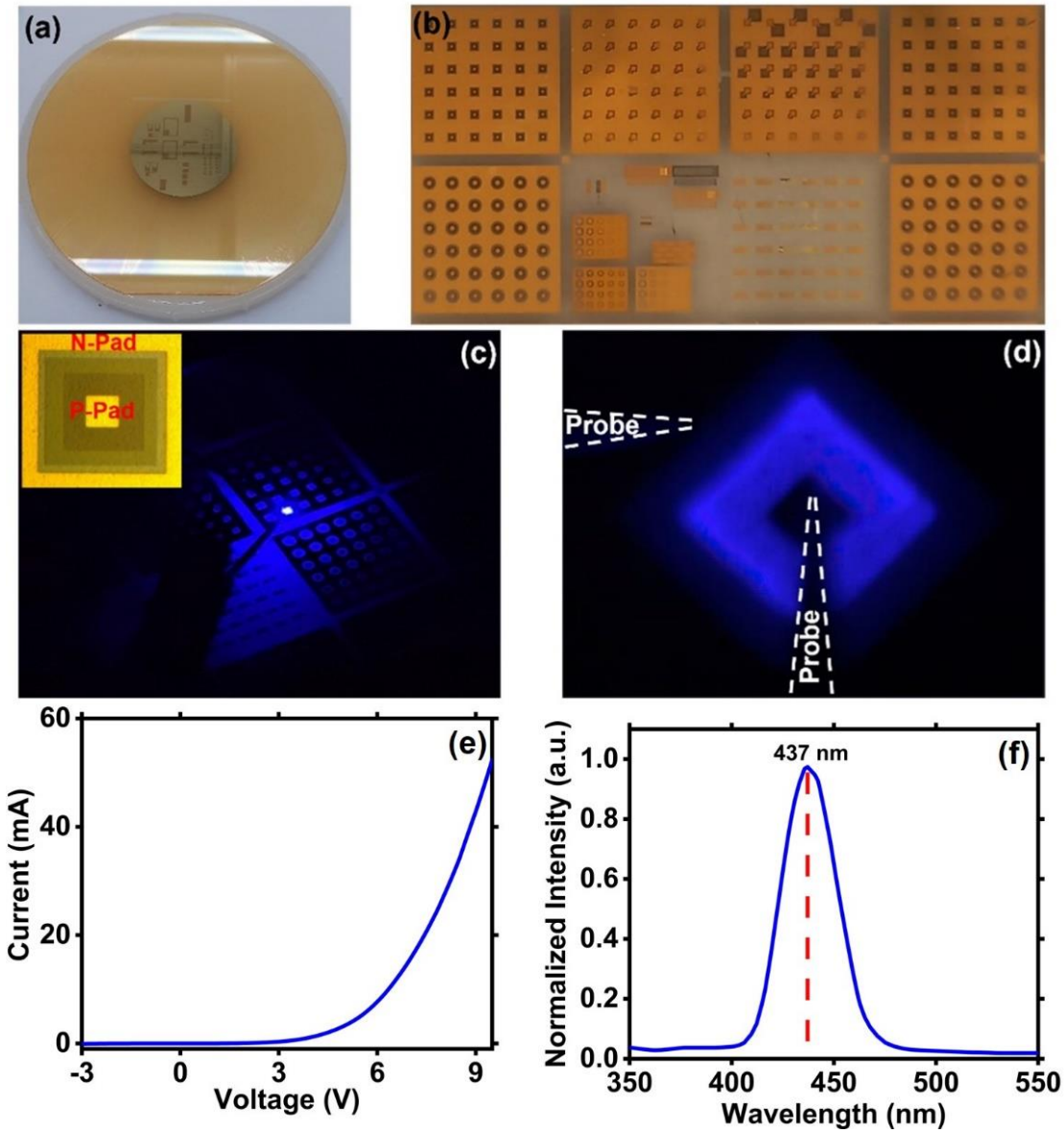

Figure 4: (a) Image showing the full 6-inch wafer at the intermediate process stage, (b) Zoomed binocular image showing the final fabricated devices, (c) Far field image of emission of light from LED. Inset in (c): top view of LED, (d) Near filed image of emission of light from LED, (e) I-V characteristics of LED on linear scale, and (f) Electroluminescence spectrum of LED.

2.4. Lift-off and transfer of fabricated LED devices on h-BN/6-inch sapphire substrate

Motivated by the results obtained in the previous section, we finally tested the lift-off and transfer of the GaN-based LED heterostructures grown on h-BN/6-inch sapphire substrate. To obtain this, the self lift-off and transfer process (SLOT) [28] was employed as shown in Fig. 5. As shown in Fig. 5a, chips of size 1 cm * 1 cm separated by photoresist were electroplated, which upon heating at 100^{o}C released off the LED heterostructure and transferred to the flexible copper carrier. These lifted-off LED heterostructures were processed to fabricate the vertical LED structures as shown in Fig. 5d and 5e. Though we limit ourselves to square of 1 cm * 1 cm, the size of the lifted off chip is limited by the shape and size of the photolithography mask. This ability to transfer the LED heterostructures enables the integration of the device into a wider range of electronic systems and applications.

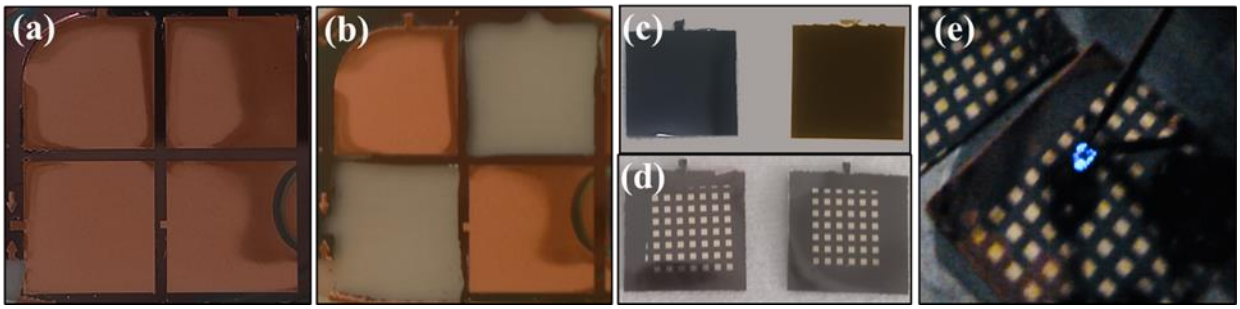

Figure 5: Image showing different steps of the SLOT process (a) Copper electroplating, (b) Self lift-off of LED heterostructures on copper, (c) Lifted-off face (n-AlGaN), (d) Vertical LEDs with front n-contact and back copper p-contact, and (e) Blue light emission from the lifted-off device.

3. Conclusions

We have successfully demonstrated the vdW epitaxy and the fabrication of blue LED devices on h-BN grown on 6-inch sapphire substrate. The fabricated LED heterostructures exhibited bright blue illumination with an electroluminescence peak at 437 nm. In addition, we have demonstrated the ability to lift-off these LED heterostructures and transfer them to a flexible copper carrier. With these results, the fabrication of GaN based LEDs on h-BN/sapphire becomes more appealing for commercialization and especially the study to avoid the delamination

developed in this paper can be applicable to larger substrates, 8-inch, 10-inch, 12-inch and beyond to respond to the scale up of the sapphire substrates production.

4. Methods

The epitaxial growth of the GaN-based LED heterostructures was performed in an Aixtron Close Coupling Showerhead (CCS) MOCVD reactor system on 6-inch sapphire substrates using H_2 and N_2 as carrier gases. The following materials were used as precursors during the growth process: Triethylboron (TEB) for boron, Trimethylgallium/Triethylgallium (TMGa/TEG) for gallium, Trimethylindium (TMIn) for indium, Trimethylaluminum (TMAl) for aluminum, and Ammonia (NH_3) for nitrogen. Silane (SiH_4) and biscyclopentadienyl-magnesium (Cp_2Mg) were used as n-type and p-type doping sources, respectively. First, a 3 nm thick h-BN layer was grown at 1280°C and 90 mbar on the 6-inch sapphire substrate. The hydrogen was used as carrier gas. The growth rate is 15 nm/hour. Further information on the specific growth conditions can be found in previous reports [17,23]. Then, a 230 nm silicon (Si) doped AlGaN layer with an Al mole fraction of 15% was grown at 1100°C, which served as an interfacial buffer between the sp^3-bonded 3D epitaxial layers and the 2D h-BN and promoted nucleation. Subsequently, a 500 nm Si doped GaN layer was then grown on top of the AlGaN buffer layer. InGaN/GaN MQWs and p-GaN were regrown on 6-inch n-GaN/n-AlGaN/h-BN/sapphire wafer templates at 700/800°C and 800°C and pressure of 300 mbar and 150 mbar, respectively. The 3 MQWs consists of 11.5 nm thick GaN barrier layers and 2.5 nm thick InGaN QW layers deduced from in-situ laser reflectometry measurements and calibrations with an In mole fraction of 12% to get light emission in the blue spectrum. Finally, 100 nm of magnesium (Mg) doped p-GaN was grown under N_2. The activation of Mg was done under N_2 at low temperature.

Scanning electron microscopy (SEM) and atomic force microscopy (AFM) were used to study the surface morphology of the samples before and after mechanical lift-off. The crystalline structure of the h-BN layer and the GaN-based LED heterostructures on h-BN epilayer was examined using high-resolution X-ray diffraction (HR-XRD) scans performed on a Panalytical X'Pert Pro Materials Research Diffractometer system with Cu Kα radiation in the triple-axis mode. Raman spectra were obtained using LabRam HR EVOLUTION Raman spectroscopy with 532 nm

laser excitation. The photoluminescence (PL) of the epilayers were measured by the white light interference and a 266 nm ultraviolet laser.

For the process of grown LED heterostructures and device fabrication, a standard lithography-based process was employed. At first mesa etch isolation was achieved using inductively coupled plasma having Cl_2/Ar chemistry. This was followed by deposition of Ti/Al/Ni/Au n-contact which was annealed at 850^{o}C for 30 seconds under N_2 atmosphere. Then Ni/Au p-contact was deposited and annealed at 600^{o}C for 60 seconds under oxygen (O_2) atmosphere. Finally, Ti/Au n-and p-pads were deposited. All the metal deposition steps were performed in electron beam evaporator. Resist stripping and metal lift-off steps were performed under static conditions by submerging samples in bath of DMSO at 80^{o}C to avoid any delamination risk.

For self lift-off and transfer process (SLOT), at first Ni/Au p-contact was deposited and annealed at 600^{o}C for 60 seconds under O_2 atmosphere. Then, a 10 nm thick Ti adhesion layer and 20 nm thick Au seed layer was deposited for cooper electroplating. Following this photolithography was performed for defining shape and size of the membranes to be lifted off. Then copper electroplating was performed using an acid free copper sulphate solution at current density of 20 mA/cm^2. Following this, the sample was heated on hot plate at 100^{o}C for 1 hour and self-lift off was achieved. Finally, array of 500 μm * 500 μm square n-contact was deposited on the n-AlGaN face of the lifted-off membranes.

The device's optoelectronic properties were assessed by measuring its current-voltage (I-V) characteristics and electroluminescence (EL) spectrum using a Keithley 4200A-SCS parameter analyzer and an Ocean Insight high-resolution spectrometer, respectively.

Acknowledgements

The authors acknowledge Dr. D. Chapron and Dr. T. Kauffmann from the Spectroscopy Platform of the LMOPS, Université de Lorraine & Centrale Supélec for their help with Raman measurements.

This study has been partially funded by the French National Research Agency (ANR), under the INMOST (Grant ANR-19-CE08-0025) project, under the GANEXT Laboratory of Excellence

(LabEx) project, and French PIA project Lorraine Université d'Excellence (Grant ANR-15- IDEX-04-LUE), as well as by the Region Grand Est in France.

Conflict of Interest

The authors declare that they have no conflict of interest.

Data Availability Statement

The data that support the findings of this study are available from the corresponding author upon reasonable request.

Keywords

Large-area MOVPE epitaxy, van der Waals epitaxy, 2D h-BN, 6-inch LED on h-BN, simple mechanical self lift-off and transfer

References

[1] A. Koma, *Journal of Crystal Growth* **1999**, *201–202*, 236.
[2] Y. Alaskar, S. Arafin, D. Wickramaratne, M. A. Zurbuchen, L. He, J. McKay, Q. Lin, M. S. Goorsky, R. K. Lake, K. L. Wang, *Adv. Funct. Mater.* **2014**, *24*, 6629.
[3] D. Liang, T. Wei, J. Wang, J. Li, *Nano Energy* **2020**, 104463.
[4] K. Reidy, J. D. Thomsen, H. Y. Lee, V. Zarubin, Y. Yu, B. Wang, T. Pham, P. Periwal, F. M. Ross, *Nano Lett.* **2022**, *22*, 5849.
[5] J. Yu, L. Wang, Z. Hao, Y. Luo, C. Sun, J. Wang, Y. Han, B. Xiong, H. Li, *Adv. Mater.* **2020**, *32*, 1903407.
[6] H. Zhou, Y. Xu, X. Chen, Y. Liu, B. Cao, W.-J. Yin, C. Wang, K. Xu, *Journal of Alloys and Compounds* **2020**, *844*, 155870.
[7] H. Chang, Z. Chen, B. Liu, S. Yang, D. Liang, Z. Dou, Y. Zhang, J. Yan, Z. Liu, Z. Zhang, J. Wang, J. Li, Z. Liu, P. Gao, T. Wei, *Advanced Science* **2020**, *7*, 2001272.
[8] Y. Kobayashi, K. Kumakura, T. Akasaka, T. Makimoto, *Nature* **2012**, *484*, 223.
[9] T. Ayari, S. Sundaram, X. Li, Y. El Gmili, P. L. Voss, J. P. Salvestrini, A. Ougazzaden, *Applied Physics Letters* **2016**, *108*, 171106.
[10] J.-H. Park, X. Yang, J.-Y. Lee, M.-D. Park, S.-Y. Bae, M. Pristovsek, H. Amano, D.-S. Lee, *Chem. Sci.* **2021**, *12*, 7713.
[11] Y. Yang, Y. Peng, M. F. Saleem, Z. Chen, W. Sun, *Materials* **2022**.
[12] A. E. Naclerio, P. R. Kidambi, *Advanced Materials* **2023**, *35*, 2207374.
[13] Y. Li, Y. Zhao, T. Wei, Z. Liu, R. Duan, Y. Wang, X. Zhang, Q. Wu, J. Yan, X. Yi, G. Yuan, J. Wang, J. Li, *Jpn. J. Appl. Phys.* **2017**, *56*, 085506.
[14] Q. Zhao, J. Miao, S. Zhou, C. Gui, B. Tang, M. Liu, H. Wan, J. Hu, *Nanomaterials (Basel)* **2019**, *9*, 1178.
[15] J. Yu, L. Wang, X. Han, Z. Hao, Y. Luo, C. Sun, Y. Han, B. Xiong, J. Wang, H. Li, *Opt. Mater. Express, OME* **2021**, *11*, 4118.
[16] J. W. Shon, J. Ohta, K. Ueno, A. Kobayashi, H. Fujioka, *Sci Rep* **2014**, *4*, 5325.
[17] X. Li, S. Sundaram, Y. El Gmili, T. Ayari, R. Puybaret, G. Patriarche, P. L. Voss, J. P. Salvestrini, A. Ougazzaden, *Crystal Growth & Design* **2016**, *16*, 3409.
[18] T. Ayari, C. Bishop, M. B. Jordan, S. Sundaram, X. Li, S. Alam, Y. ElGmili, G. Patriarche, P. L. Voss, J. P. Salvestrini, A. Ougazzaden, *Scientific Reports* **2017**, *7*.

[19] T. Ayari, S. Sundaram, X. Li, S. Alam, C. Bishop, W. El Huni, M. B. Jordan, Y. Halfaya, S. Gautier, P. L. Voss, J. P. Salvestrini, A. Ougazzaden, *ACS Photonics* **2018**, *5*, 3003.
[20] S. Sundaram, P. Vuong, A. Mballo, T. Ayari, S. Karrakchou, G. Patriarche, P. Voss, J. Salvestrini, A. Ougazzaden, *APL Materials* **2021**, *9*, 061101.
[21] J. Shin, H. Kim, S. Sundaram, J. Jeong, B.-I. Park, C. S. Chang, J. Choi, T. Kim, M. Saravanapavanantham, K. Lu, S. Kim, J. M. Suh, K. S. Kim, M.-K. Song, Y. Liu, K. Qiao, J. H. Kim, Y. Kim, J.-H. Kang, J. Kim, D. Lee, J. Lee, J. S. Kim, H. E. Lee, H. Yeon, H. S. Kum, S.-H. Bae, V. Bulovic, K. J. Yu, K. Lee, K. Chung, Y. J. Hong, A. Ougazzaden, J. Kim, *Nature* **2023**, *614*, 81.
[22] P. Vuong, A. Mballo, S. Sundaram, G. Patriarche, Y. Halfaya, S. Karrakchou, A. Srivastava, K. Krishnan, N. Y. Sama, T. Ayari, S. Gautier, P. L. Voss, J. P. Salvestrini, A. Ougazzaden, *Appl. Phys. Lett.* **2020**, *116*, 042101.
[23] P. Vuong, S. Sundaram, V. Ottapilakkal, G. Patriarche, L. Largeau, A. Srivastava, A. Mballo, T. Moudakir, S. Gautier, P. L. Voss, J.-P. Salvestrini, A. Ougazzaden, *ACS Appl. Nano Mater.* **2022**, *5*, 791.
[24] L. Ravi, M. A. Rather, K.-L. Lin, C.-T. Wu, T.-Y. Yu, K.-Y. Lai, J.-I. Chyi, *ACS Appl. Electron. Mater.* **2023**, *5*, 146.
[25] T. Vodenitcharova, L. C. Zhang, I. Zarudi, Y. Yin, H. Domyo, T. Ho, *IEEE Trans. Semicond. Manufact.* **2006**, *19*, 449.
[26] Engineering ToolBox, (2018). Hydrogen - Thermal Conductivity vs. Temperature and Pressure. Available at: *https://www.engineeringtoolbox.com/hydrogen-H2-thermal-conductivity-temperature-pressure-d_2106.html*
[27] Engineering ToolBox, (2018). Nitrogen - Thermal Conductivity vs. Temperature and Pressure. Available at: *https://www.engineeringtoolbox.com/nitrogen-N2-thermal-conductivity-temperature-pressure-d_2084.html*
[28] S. Karrakchou, S. Sundaram, R. Gujrati, P. Vuong, A. Mballo, H. E. Adjmi, V. Ottapilakkal, W. El Huni, K. Bouzid, G. Patriarche, A. Ahaitouf, P. L. Voss, J. P. Salvestrini, A. Ougazzaden, *ACS Appl. Electron. Mater.* **2021**, *3*, 2614.